Cooperative Effects of RIG-I-like Receptor Signaling and IRF1 on DNA Damage-Induced Cell Death

David Y. Zander[1,2], Sandy S. Burkart[1,3], Sandra Wüst[1], Vladimir G. Magalhães[1], Marco Binder[1,§]

[1]Research Group "Dynamics of Early Viral Infection and the Innate Antiviral Response", Division Virus-Associated Carcinogenesis, German Cancer Research Center, Heidelberg, Germany

[2]Department of Infectious Diseases, Molecular Virology, Heidelberg University, Heidelberg, Germany

[3]Faculty of Biosciences, Heidelberg University, Heidelberg, Germany

[§]Corresponding author: m.binder@dkfz.de

Abstract

Properly responding to DNA damage is vital for eukaryotic cells, including the induction of DNA repair, growth arrest and, as a last resort to prevent neoplastic transformation, cell death. Besides being crucial for ensuring homeostasis, the same pathways and mechanisms are at the basis of chemoradiotherapy in cancer treatment, which involves therapeutic induction of DNA damage by chemical or physical (radiological) measures. Apart from typical DNA damage response mediators, the relevance of cell-intrinsic antiviral signaling pathways in response to DNA breaks has recently emerged. Originally known for combatting viruses via expression of antiviral factors including IFNs and establishing of an antiviral state, RIG-I-like receptors (RLRs) were found to be critical for adequate induction of cell death upon the introduction of DNA double-strand breaks. We here show that presence of IRF3 is crucial in this process, most likely through direct activation of pro-apoptotic factors rather than transcriptional induction of canonical downstream components, such as IFNs. Investigating genes reported to be involved in both DNA damage response and antiviral signaling, we demonstrate that IRF1 is an obligatory factor for DNA damage-induced cell death. Interestingly, its regulation does *not* require activation of RLR signaling, but rather sensing of DNA double strand breaks by ATM and ATR. Hence, even though independently regulated, both RLR signaling and IRF1 are essential for proper induction/execution of intrinsic apoptosis. Our results not only support more broadly developing IRF1 as a biomarker predictive for the effectiveness of chemoradiotherapy, but also suggest investigating a combined pharmacological stimulation of RLR and IRF1 signaling as a potential adjuvant regimen in tumor therapy.

Introduction

DNA damage is a ubiquitous and existential threat to organisms. Potential causes comprise ionizing radiation (IR), genotoxic chemicals, but also cell-intrinsic mechanisms. Among various possible DNA alterations, the most drastic and impactful are DNA double-strand breaks (DSBs). Complex mechanisms involving detection by ATM, ATR, and downstream processes including the tumor suppressor p53 and checkpoint inhibition, either lead to sufficient repair of the damage or to induction of programmed cell death [1, 2]. The latter mostly comprises apoptosis, but other forms such as necroptosis and pyroptosis have recently been reported as well. Mutations of the central DSB sensors can cause severe diseases such as ataxia telangiectasia, associated with carcinogenesis and serious immunodeficiency [3-5]. Originally discovered and best-studied in the context of the antiviral innate immune response, IRF1 has been implicated in the DNA damage response and tumor suppressor functions [6-9].

Following the IRF1 example, it became apparent that cell-intrinsic antiviral signaling pathways also substantially contribute to DNA damage-induced cell death. Both STING and RIG-I-like receptor (RLR) pathways detect damage-associated molecular patterns (DAMPs), such as endogenous DNA fragments and nuclear RNA, and can trigger cell death [10, 11]. Previously, RIG-I stimulation has been

shown to induce death of breast cancer cells, putting forward a potential application in tumor therapy [12]. Typically, the RLRs, RIG-I and MDA5, are stimulated by non-self RNA in the event of viral infection. Interaction with their adaptor MAVS leads to activation of the transcription factors IRF3, NF-κB p65/RELA and p50/NFKB1. The resulting expression of ISGs and IFNs of type I/III causes the establishment of an antiviral state and, in most cases, effective containment of the invading pathogen. In addition to apoptosis sensitizing effects of NF-κB and IFNs through expression of pro-apoptotic factors, direct cell death mediating effects have recently been reported for MAVS and IRF3 [13, 14]. Chattopadhyay et al. were first to identify and characterize the RLR-induced IRF3-mediated pathway of apoptosis (RIPA) [15]. Stimulation of RLRs with dsRNA or viral infection induces MAVS-dependent ubiquitination of IRF3 and subsequent activation of pro-apoptotic factors independent of IRF3's transcriptional activity [16]. Furthermore, MAVS was shown to directly interact with procaspase-8, forming so-called MAVS-death-inducing signaling complexes upon viral infection [17]. Here we show that RLR signaling, IRF1, and canonical DNA damage response pathways, comprising ATM/ATR and p53, are essential for efficient induction of apoptosis. We show that these pathways have independent pro-apoptotic capacities, and we present new insights into IRF1's complex cellular functions.

Methods

Cell culture, cell line generation, and stimulation. Cell lines were grown at 37 °C, 95 % humidity, and 5 % CO_2 in Dulbecco's modified eagle medium (DMEM high glucose, Life Technologies, Carlsbad, CA, USA), supplemented with final 10 % (v/v) fetal calf serum (FCS, Thermo Fisher Scientific, Waltham, MA, USA), 1x non-essential amino acids (Thermo Fisher Scientific), and 100 U/ml penicillin and 100 ng/ml streptomycin (LifeTechnologies). For generation of transgene expressing A549 cell lines by lentiviral transduction, lentiviral particles were produced by transfecting HEK 293T cells with plasmids pCMV-dr8.91, pMD2.G, and the respective retroviral vector (pWPI) using calcium phosphate transfection (CalPhos Mammalian Transfection Kit, Takara Bio Europe, Saint-Germain-en-Laye, France). After two days the supernatant was harvested, sterile filtered, and used to transduce target cells two times for 24 h. Transduced cells were selected with antibiotics appropriate for the encoded resistance gene (5 µg/ml blasticidin, MP Biomedicals, Santa Ana, CA, USA; 1 µg/ml puromycin, Sigma Aldrich; 1 mg/ml geneticin (G418), Santa Cruz, Dallas, TX, USA). Knockout (KO) cell lines were generated by clustered regularly interspaced short palindromic repeats (CRISPR)/Cas9 technology. DNA oligonucleotides coding for guideRNAs against the respective genes (sequences shown in Supplementary Table S1) were cloned into the expression vector LentiCRISPRv2 (Feng Zhang, Addgene #52961).

Transduced A549 wild-type cells were selected with puromycin, single cell clones were isolated, and KO was validated by immunoblotting and functional tests (Fig. S5). A549 *IFNAR1*$^{-/-}$ *IFNLR1*$^{-/-}$ *IFNGR*$^{-/-}$ (IFNR TKO), *IRF1*$^{-/-}$, *IRF1* OE, *IRF3*$^{-/-}$, IRF3-eGFP H2B-mCherry, *MAVS*$^{-/-}$, *MYD88*$^{-/-}$, *RELA*$^{-/-}$, and

86 *RIG-I*$^{-/-}$ were reported previously [18-22]. A549 *RIG-I* OE cells were generated by stable lentiviral
87 transduction as described previously [19]. Cells transduced with non-targeting gRNA (sequence taken
88 from the GeCKO CRISPR v2 library) were used as controls. PH5CH non-neoplastic hepatocytes and
89 HepG2 cells were kindly provided by Dr. Volker Lohmann (Heidelberg University, Heidelberg,
90 Germany). Huh7.5 cells were generously provided by Dr. Charles Rice (Rockefeller University, New
91 York).
92 Stimulation was performed with doxorubicin (DOX, Hölzel Diagnostika, Cologne, Germany),
93 etoposide (ETO, Cell Signaling Technology, Danvers, MA, USA), or cells were transfected with *in*
94 *vitro* transcribed and chromatographically purified 200 bp 5'ppp-dsRNA [23], poly(C) (Sigma-
95 Aldrich), and poly(I:C) (Sigma-Aldrich) using Lipofectamine 2000 (Invitrogen, Carlsbad, CA, USA)
96 following the manufacturer's protocol. Cells were γ-irradiated with doses of 0-30 Gy using a
97 Gammacell 40 Exactor (Best Theratronics, Ottawa, Canada).
98 **Real-time imaging of cell death.** A549 cells stably expressing histone H2B mCherry [21] were seeded
99 at density of 2 x 10^3 cells per 96-well. The next day, cells were stimulated with 1-2 µM DOX (10 h),
100 25 µM ETO (10 h), 0.1 ng/ml dsRNA (8 h), or γ-IR. DMSO (Carl Roth, Karlsruhe, Germany), poly(C),
101 and mock irradiation were used as appropriate controls. Post treatment, fresh medium was
102 supplemented with 1:10 000 IncuCyte® Cytotox Green Reagent (Sartorius, Göttingen, Germany) to
103 determine dead cells. Total cell number and dead cells were monitored every 2 h using a 10x
104 magnification in an IncuCyte® S3 Live-Cell Analysis System (Satorius, Göttingen, Germany). For IFN
105 pre-stimulation, 200 IU/ml IFN-β (IFN-β1, Bioferon, Laupheim, Germany) or IFN-γ (R&D Systems,
106 Minneapolis, MN, USA) were added at the time of seeding. For inhibitor administration, 40 µM Z-
107 VAD-FMK (Z-VAD, R&D Systems) and 10 µM Necrostatin-7 (Nec-7, Sigma Aldrich), or 25 µM
108 TPCA-1 (Sigma Aldrich) were added 2 h prior treatment. IncuCyte® Software (2019B Rev2, Satorius,
109 Göttingen, Germany) was used to mask cells in phase contrast images. Calculations were performed
110 applying the following settings: red fluorescence: segmentation top-hat, radius 100 µM, threshold
111 (GCU) 0.4, edge split sensitivity -35, area 60-1000 μm^2, integrated intensity ≥ 60; green fluorescence:
112 segmentation top-hat, radius 100 µM, threshold (GCU) 10, edge split sensitivity -40, area 100-700 μm^2,
113 eccentricity ≤ 0.8, mean intensity 7-1000, integrated intensity ≥ 2500. Percentage of dead cells was
114 calculated relative to total cell count. Data represent the results of at least three biologically independent
115 experiments. For curve charts, results were normalized to the control cell line of each replicate. Bars
116 represent non-normalized means 36 h post treatment.
117 **Immunofluorescence microscopy and determination of cellular IRF3 distribution.** Fluorescence
118 microscopy was performed to visualize phosphorylated histone H2A.X. After 4 h treatment with 2 µM
119 DOX or DMSO, or 1 h post γ-IR with 20 Gy or 0 Gy, cells were permeabilized with -20 °C methanol
120 and fixed with 4 % paraformaldehyde. To block non-specific background, cells were incubated with
121 1 % (w/v) bovine serum albumin (BSA) and 10 % (v/v) FCS for 30 min. Primary antibodies specific
122 for phospho-H2A.X (Cell Signaling Technology, 9718, 1:1000) were applied at 4 °C over-night. Slides

123 were incubated with Alexa Fluor® 488 anti-rabbit (ThermoFisher Scientific, Waltham, MA, USA,
124 A11008, 1:1000) and DAPI (ThermoFisher Scientific, D1306, 1:5000) for 1 h. For determination of
125 cellular IRF3 distribution, A549 cells stably expressing IRF3-eGFP and histone H2B-mCherry were
126 stimulated either with DOX or poly(I:C) for 12 h. Fluorescence was visualized using a Primovert
127 microscope (Carl Zeiss, Jena, Germany).
128 **Immunoblotting.** Stimulated cells were lysed in Laemmli sample buffer, and digested with Benzonase®
129 Nuclease (Merck Millipore, Burlington, MA, USA). For inhibitor administration, 20 µM KU-55933
130 (Sigma-Aldrich), 25 µM Rabusertib (Hölzel Diagnostika), 25 µM TPCA-1 (Sigma Aldrich), or 10 µM
131 VE-822 (Hölzel Diagnostika) were added 2 h prior treatment. For stimulation with IFNs, 200 IU/ml
132 IFN-α (PBL Assay Science, Piscataway, NJ, USA), IFN-β, or IFN-γ were applied over-night. Lysed
133 samples were further denatured at 95 °C for 5 min and cleared from detritus. Resulting protein extracts
134 were subjected to 10 % (w/v) SDS-polyacrylamide gel electrophoresis and transferred to PVDF
135 membranes (Bio-Rad, Hercules, CA, USA, 0.2 µm pore size). Upon incubation with 5 % (w/v) BSA
136 for 2 h to block non-specific background, membranes were probed using antibodies specific for β-actin
137 (Sigma-Aldrich, A5441, 1:5000), calnexin (Enzo Biochem, Farmingdale, NY, USA, ADI-SPA-865-F,
138 1:1000), CASP3 (Cell Signaling Technology, 9662S, 1:1000), CASP9 (Cell Signaling Technology,
139 9508, 1:1000), IRF1 (Cell Signaling Technology, 8478S, 1:1000), phospho-IRF3 (pS396,
140 ThermoFisher Scientific, MA5-14947, 1:1000), JAK1 (Cell Signaling Technology, 3332S, 1:1000),
141 MDA5 (Enzo Biochem, ALX-210-935, 1:1000), NFKB1 (p50) (Abcam, Cambridge, UK, ab32360,
142 1:1000), p53 (Santa Cruz Biotechnology, Dallas, TX, USA, sc-126, 1:1000), or STAT1 (BD
143 Biosciences, Franklin Lakes, NJ, USA, 610115, 1:1000) at 4 °C over-night. For detection, anti-rabbit
144 horseradish peroxidase (HRP) (Sigma-Aldrich, A6154-5X1ML, 1:20 000) or anti-mouse HRP (Sigma-
145 Aldrich, A4416-5X1ML, 1:10 000) were applied for 1 h, membranes were covered with Amersham
146 ECL Prime Western Blotting Detection Reagent (ThermoFisher Scientific) for 1 min, and luminescence
147 was detected using a sensitive CCD camera system (ECL ChemoCam Imager 3.2, INTAS Science
148 Imaging Instruments, Göttingen, Germany). Densitometric analysis of the protein bands was performed
149 using ImageJ (1.52e). Data shown represent the results of at least three biologically independent
150 experiments.
151 **Quantitative PCR with reverse transcription (qRT-PCR).** Upon stimulation, cells were lysed and
152 total RNA was isolated with the Monarch RNA isolation kit (New England Biolabs, Ipswich, MA,
153 USA), following the manufacturer's protocol. After extraction, complementary DNA (cDNA) was
154 generated using the High Capacity cDNA Reverse Transcription kit (ThermoFisher Scientific).
155 Determination of messenger RNA (mRNA) expression was performed using iTaq Universal SYBR®
156 Green Supermix (Bio-Rad) on a CFX96 real-time-system (Bio-Rad). Sequences of specific exon-
157 spanning PCR primers are shown in Supplementary Table S2. GAPDH mRNA was used as a
158 housekeeping gene control and relative expression determined by $2^{\Delta Ct}$ (thus, not normalizing to
159 reference condition).

160 **Cell Viability.** A549 cells were seeded at a density of 6 x 10^3 cells per 96-well. Upon treatment with
161 2 µM DOX or DMSO for 24 h, cell viability was determined using the CellTiter-Glo® luminescent cell
162 viability assay (Promega, Madison, WI, USA) following the manufacturer's protocol. Luciferase
163 activity was measured using a Mithras LB 943 multimode reader (Berthold Technologies, Bad Wildbad,
164 Germany).
165 **Caspase activity.** A549 cells were seeded at density of 6 x 10^3 cells per 96-well. 48 h post treatment
166 with 0-2 µM DOX for 10 h, caspase-3/7 activity was determined using the Apo-ONE® homogeneous
167 caspase-3/7 assay (Promega) following the manufacturer's instructions. Resulting fluorescence was
168 measured using the Mithras LB 943 multimode reader (Berthold Technologies).
169 **Statistics**
170 Comparison of datasets was performed using a paired, two-tailed Student's t-test. * indicates $p \leq 0.05$,
171 ** $p \leq 0.01$, *** $p \leq 0.001$, **** $p \leq 0.0001$. Error bars represent standard deviation.

172 ## Results

173 **Apoptosis induction via DNA damage response pathway in A549 cells**
174 To investigate the molecular links between DNA damage-induced cell death and innate immune
175 signaling, we used immunocompetent A549 human lung carcinoma cell lines with functional knockouts
176 (KOs) of components of both pathways. Cells were treated with DNA DSB inducers, specifically γ-IR
177 or the topoisomerase II inhibitors doxorubicin (DOX) and etoposide (ETO), and the resulting cell death
178 was monitored on single-cell level by real-time imaging.
179 Treatment of A549 cells with DOX resulted in pronounced cell death (Fig. 1A) and a corresponding
180 reduction of bulk cell viability (Fig. 1B), accompanied by the detection of the DNA damage marker
181 phospho-histone H2A.X by immunofluorescence (Fig. 1C). As in DMSO control conditions no cell
182 death was observed (Fig. 1A), for the clarity of presentation we omitted this control in the following
183 figures (data was acquired in every experiment). In order to characterize the type of cell death
184 predominant upon DOX-induced DNA damage, we first evaluated activation of caspase-3 and -7 being
185 pivotal markers of apoptosis. DOX treatment activated caspase-3 and -7 in a dose-dependent manner
186 (Fig. 1D). Conversely, we treated cells with the pan-caspase inhibitor Z-VAD, or depleted caspase-3 or
187 -9. Both approaches resulted in a significant reduction of cell death upon DOX treatment (Fig. 1E, F,
188 H). These findings confirmed prior reports that cell death driven by DOX is mainly due to apoptosis
189 [24]. Next, we investigated typical components of the DNA damage response upstream of caspase
190 activation. In line with p53's (*TP53*) essential role in inducing apoptosis, depletion of p53 showed a
191 significant reduction of cell death (Fig. 1G, H). Interestingly, *TP53*$^{-/-}$ had the opposite effects at late
192 time points, elevating cell death for time points >54 h (Fig. 1G). Amongst others, p53 induces apoptosis
193 via activation of PUMA and NOXA. Accordingly, we found *PUMA* and *NOXA* transcript levels to be
194 increased in DOX treated cells (Fig. 1I), supporting a canonical DNA damage response through p53 in
195 DOX-treated A549 cells.

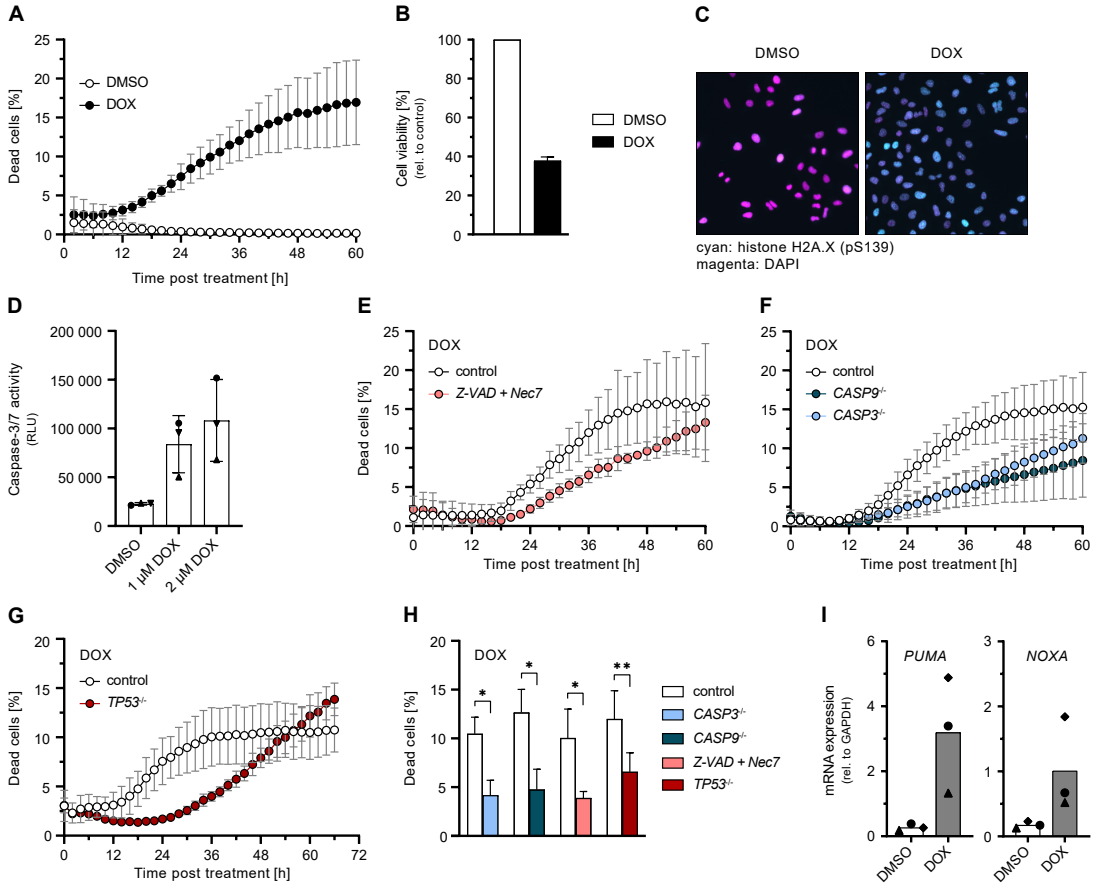

Fig. 1. Induction of apoptosis upon DOX-mediated DNA damage.

(**A**) Percentage of dead A549 cells relative to total cells counted over time post DOX or DMSO treatment. **(B)** Cell viability of A549 cells post DOX treatment for 24 h. **(C)** Immunofluorescence of phosphorylated histone H2A.X (S139) (cyan) and DAPI-stained nuclei (magenta) in A549 cells post DOX treatment for 4 h. **(D)** Caspase-3/7 activity of A549 cells 24 h post DOX treatment for 10 h. **(E-H)** Percentage of dead A549 cells with caspase inhibition or functional KO of the indicated genes relative to total cells counted over time **(E-G)** or 36 h **(H)** post DOX treatment. **(I)** A549 cells were treated with 1 µM DOX or DMSO for 24 h. PUMA and NOXA mRNA transcripts were determined by qRT-PCR. (**A, B, D-I**) Data shown represent the results of at least three biologically independent experiments.

Relevance of innate antiviral immunity pathways in DNA damage induced cell death

In order to investigate the contribution of antiviral signaling cascades to the induction of DSB-induced cell death, we compared the impact of the major antiviral pathways using KOs of their respective signaling adapters. We observed DOX-induced cell death to be significantly reduced only by MAVS depletion (RLR signaling), but not so in the absence of STING (cGAS signaling), TRIF (TLR3 signaling), or MYD88 (general TLR signaling) (Fig. 2A-C). Despite RLR signaling appeared to play a major role, neither canonical IRF3 phosphorylation nor its nuclear translocation could be detected

214 (Fig. 2D, E). Consistently, there was also no characteristic RLR-mediated induction of ISGs, such as
215 *IFIT1* (Fig. 2F).

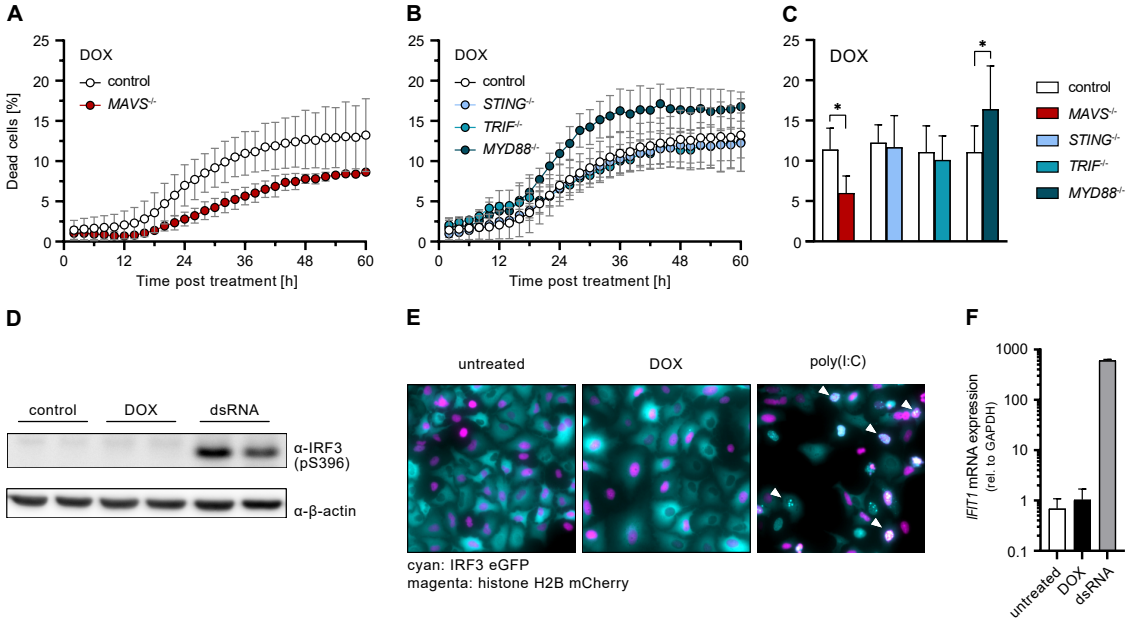

216

217 **Fig. 2. Relevance of antiviral signaling adapters and ISG response during DOX-induced DNA damage**
218 **response.**
219 (**A-C**) Percentage of dead A549 cells with functional KO of the indicated genes relative to total cells counted over
220 time **(A, B)** or 36 h **(C)** post DOX treatment. **(D)** A549 cells were stimulated with 1 µM DOX or 1 ng/ml dsRNA
221 for 8 h. Phosphorylated IRF3 (S396) was determined by western blot. **(E)** A549 cells were stimulated with 1 µM
222 DOX or 2 µg/ml poly(I:C) for 12 h. Cellular distribution of IRF3 eGFP (cyan) and histone H2B (magenta) was
223 visualized by immunofluorescence microscopy. **(F)** A549 cells were stimulated with 1 µM DOX or 10 ng/ml
224 dsRNA for 24 h. IFIT1 mRNA transcripts were determined by qRT-PCR. (**A-C, F**) Data shown represent the
225 results of at least three biologically independent experiments.
226

227 Given the observed relevance of MAVS in DOX-induced cell death, we further analysed the effect of
228 specific RLR depletion. Both *RIG-I*$^{-/-}$ and *MDA5*$^{-/-}$ reduced cell death upon DOX treatment, however,
229 RIG-I exhibited a considerably stronger effect (Fig. 3A, C). Reciprocally, *RIG-I* overexpression (OE)
230 markedly increased cell death upon DOX treatment (but not in untreated conditions, compare Fig. S1A),
231 underlining the decisive role of RLR signaling in this process (Fig. 3B, C). In order to determine the
232 factors responsible for mediating cell death downstream of MAVS, we further examined the influence
233 of transcription factors IRF3 and NF-κB p65/RELA. We observed that depletion of either factor
234 significantly reduced DOX-induced cell death (Figure 3D, F). Using IFN-"blind" A549 *IFNAR1*$^{-/-}$
235 *IFNLR1*$^{-/-}$ *IFNGR*$^{-/-}$ (IFNR TKO) cells, we demonstrated that this effect was independent of a response
236 mediated by secreted IFNs (Fig. 3E, F), which was further confirmed using *STAT1*$^{-/-}$ cells (Fig. S1B).
237 This was in accordance with the lack of ISG expression observed previously (Fig. 2F). Thus, IRF3

238 appears to have death sensitizing effects distinct from its classical transcriptional activity in the antiviral
239 program.
240 Taken together, we demonstrated that RLR signaling is required for the induction of cell death after
241 DNA damage and that this function is independent of IFN secretion and the induction of canonical
242 ISGs.

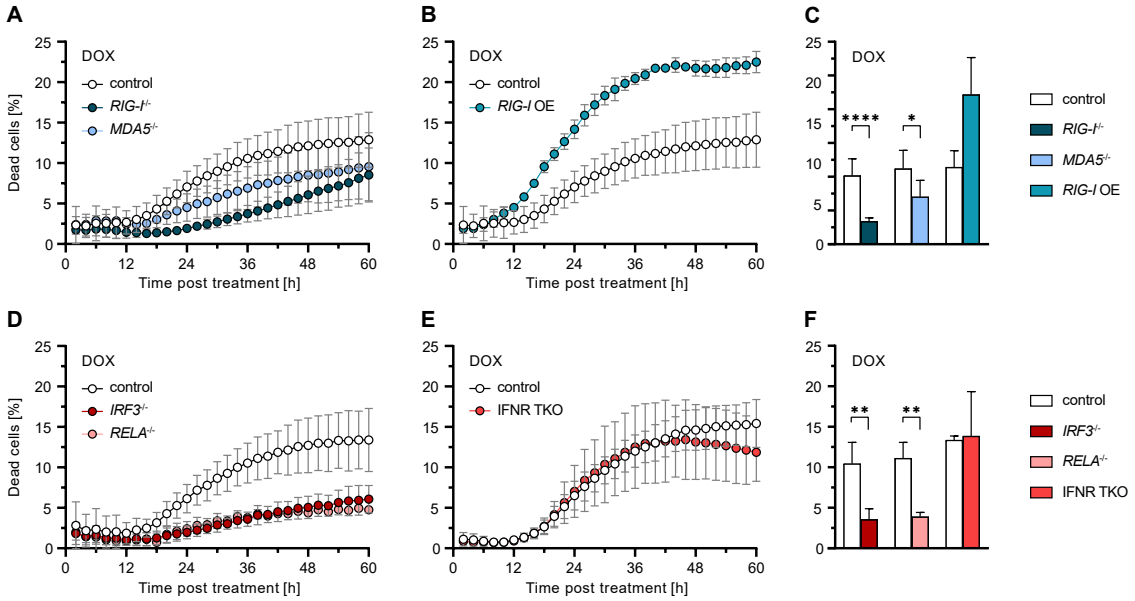

243
244 **Fig. 3. Implications of RLR signaling components and IFN signaling on DOX-induced apoptosis.**
245 **(A-F)** Percentage of dead A549 cells with functional KO or OE of the indicated genes relative to total cells counted
246 over time **(A, B, D, E)** or 36 h **(C, F)** post DOX treatment. Data shown represent the results of at least three
247 biologically independent experiments.
248
249 **Role of IRF1 in DNA damage induced apoptosis**
250 Another transcription factor of the IRF family important for antiviral defenses [6, 18], IRF1, has
251 previously also been implicated with the DNA damage response [25]. We hypothesized that upon
252 genotoxic insult, IRF1 might be a downstream target of the RLR/IRF3 pathway, as reported for virus
253 infection, and thereby link RLR activity to the DNA damage response. Indeed, upon DOX treatment,
254 we observed IRF1 upregulation at the mRNA (Fig. 4A) and protein level (Fig. 4B). Of note, *IRF1*
255 induction occurred independently of the presence of p53 (Fig. 4B). In order to determine the relevance
256 of IRF1 to cell death, we next tested *IRF1*$^{-/-}$ cells in DOX treatment. Strikingly, IRF1 depletion almost
257 completely abolished DOX-induced cell death (Fig. 4E, H). Conversely, increasing IRF1 abundance,
258 either by OE through stable transduction or by pre-stimulation of cells with IFN-β or IFN-γ, markedly
259 increased cell death upon DOX treatment (Fig. 4E, F, H), and the percentage of dead cells correlated
260 with IRF1 levels in western blot (Fig. 4C, D). Notably, neither IFN stimulation alone, nor DOX
261 treatment in IFN-primed but IRF1-depleted cells did induce cell death (Fig. S2A, B). Surprisingly, the
262 same phenotype was observed in *RIG-I*$^{-/-}$ conditions (Fig. S2C), in which IRF1 was present, suggesting

263 a strict requirement of both RLR signaling and *IRF1* induction for proper triggering and/or execution
264 of apoptosis. Similar observations were also made after ETO treatment (Fig. S2D, E), ruling out DOX-
265 specific effects.
266 The fundamental importance of IRF1 was additionally demonstrated in response to γ-IR. Although
267 irradiation did induce DNA damage in A549 cells (Fig. S2F), we could neither observe induction of
268 *IRF1* expression nor any cell death upon administration of up to 30 Gy (Fig. 4G-I). Strikingly, induction
269 of cell death upon γ-IR was restored under conditions of elevated IRF1 levels, such as stable OE or
270 IFN-γ pre-stimulation (Fig. 4G, H). In line with this, cells in which γ-IR naturally leads to an
271 upregulation of *IRF1* expression, such as PH5CH cells, did exhibit a dose-dependent induction of cell
272 death (Fig. S2G, H).
273 Thus, we showed that besides p53 and RLR signaling, IRF1 is essential for proper triggering of cell
274 death upon DNA damage. IFNs, in particular IFN-γ, sensitize cells for DNA damage-induced apoptosis
275 through upregulation of IRF1.

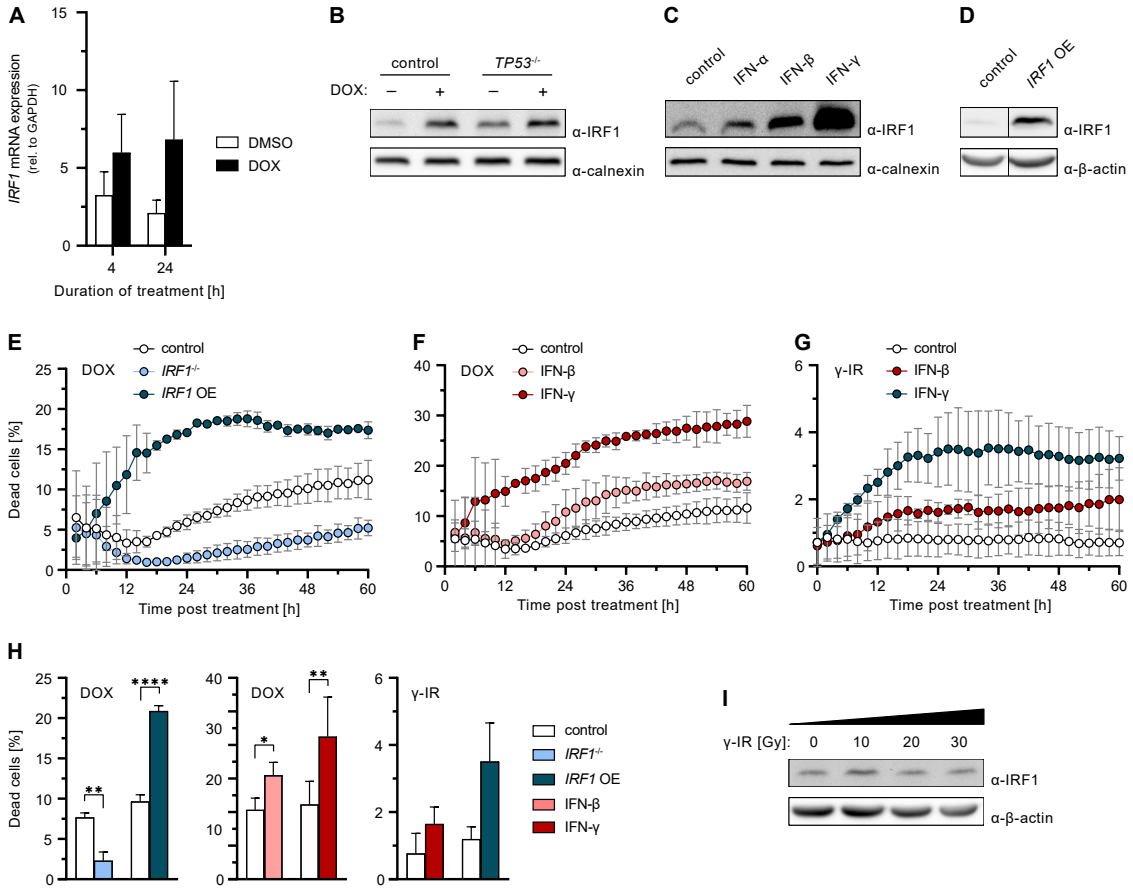

276
277 **Fig. 4. Relevance of IRF1 on DNA damage-induced cell death.**
278 **(A)** A549 cells were treated with 1 µM DOX or DMSO for 10 h. IRF1 mRNA transcripts were determined by
279 qRT-PCR. **(B)** A549 cells were treated with 1 µM DOX or DMSO for 10 h. Levels of IRF1 were determined by
280 western blot. **(C)** A549 cells were stimulated with IFN-α, IFN-β, or IFN-γ over-night. Levels of IRF1 were
281 determined by western blot. (**D**) Levels of IRF1 in A549 control and *IRF1* OE cells were determined by western

282 blot. **(E-H)** Percentage of dead A549 cells with functional KO or OE of IRF1, or post IFN pre-stimulation relative
283 to total cells counted over time (**E-G**) or 36 h (**H**) post DOX or γ-IR (20 Gy) treatment. **(I)** A549 cells were γ-
284 irradiated. After 10 h IRF1 protein levels were determined by western blot. (**A, E-H**) Data shown represent the
285 results of at least three biologically independent experiments.
286

287 **Regulation of *IRF1* expression upon DNA damage**

288 Above we have shown that RLR/IRF3 signaling as well as expression of *IRF1* are crucially important
289 for DNA damage-induced cell death. We further found IRF1 to be consistently induced under all tested
290 conditions of DNA damage leading to cell death. We now aimed to confirm whether IRF1 is in fact
291 induced as a downstream target of RLR signaling. We first investigated the induction of *IRF1*
292 expression after RIG-I stimulation using dsRNA as a canonical, highly specific agonist [23]. Indeed,
293 we observed a fully RLR-dependent (RIG-I, MAVS, IRF3) increase of IRF1 levels, with a partial
294 contribution of p65/RELA and IFN signaling (IFNR TKO) (Fig. 5A), in line with a recent report of our
295 lab [18]. dsRNA-stimulation furthermore also led to the induction of cell death, which was fully
296 abolished upon depletion of the RLR signaling components RIG-I, MAVS, or IRF3 (Fig. 5B, D).
297 Depletion of p65/RELA and the IFN receptors (IFNR TKO) had minor pro-survival effects, suggesting
298 a major role for transcription-independent RIPA with a possible but limited role for IFN signaling and
299 ISG induction (Fig. 5C, D). Interestingly and in clear contrast to the situation upon DNA damage,
300 dsRNA-induced cell death was independent of IRF1 (Fig. 5C). Nonetheless, experimentally elevating
301 IRF1 levels markedly increased the percentage of dead cells also in this setting (Fig. S3A, B).
302 These findings confirmed that, despite not being essential for cell death induction, IRF1 is induced
303 downstream of RLR signaling, at least when stimulated by a strong RIG-I specific agonist. We next
304 investigated whether this would be also the case in the context of DNA damage. Unexpectedly, upon
305 treatment of cells with DOX, induction of *IRF1* expression was neither affected by depletion of RLR
306 nor of IFN signaling components, including JAK1 (Fig. 5E, F; Fig. S3C). This suggested *IRF1*
307 expression is induced independently of and coincidentally with antiviral RLR signaling upon DNA
308 damage. We therefore hypothesized sensing of DNA damage might directly induce *IRF1*. To test this,
309 we treated cells with specific inhibitors of the prototypical DSB sensors ATM and ATR, as well as
310 potential downstream pathways. We found *IRF1* induction upon DOX-treatment to be completely
311 blocked by the ATM inhibitor KU-55933 [26] and the ATR inhibitor VE-822 [27], suggesting important
312 roles of these sensors in activation of IRF1 (Fig. 5G; Fig. S3D).
313 As *IRF1* expression has previously been shown to be NF-κB sensitive [28], we employed the common
314 pan-NF-κB and JAK1 inhibitor TPCA-1 [29, 30]. Remarkably, TPCA-1 treatment completely
315 prevented the induction of *IRF1* expression upon DOX treatment, and even strongly diminished basal
316 expression (Fig. 5G, Fig. S3D). This effect could further be confirmed upon RLR-stimulation with
317 dsRNA (Fig. S4A) and even upon IFN-γ treatment, which is a strong and well-studied canonical inducer
318 of *IRF1* (Fig. S4B). We could rule out a cell line (A549) specific effect by testing three other human

cell lines, PH5CH, HeLa and Huh7.5 (Fig. S4C). To our knowledge, this striking effect of TPCA-1 on *IRF1* expression has not been reported before. Again, corroborating IRF1's crucial role in DNA damage-induced apoptosis, supressing *IRF1* induction by TPCA-1 also reduced cell death in DOX-treated A549, PH5CH, HeLa, and Huh7.5 cells (Fig. S4D).

Finally, we aimed to identify which signaling pathway and NF-κB subunit would be responsible for *IRF1* expression upon triggering the DNA damage response. As reported in literature, ATR may signal through CHK1 to activate p50/NFKB1, a potential target of TPCA-1 [31, 32]. We therefore inhibited CHK1 by Rabusertib [33] prior to DOX-treatment. However, our experiments did not reveal any effect of CHK1 inhibition or p50/NFKB1 depletion on IRF1 levels (Fig. 5G; Fig. S3D, E). We hence conclude that a so far elusive pathway downstream of the ATM/ATR system induces *IRF1*.

Taken together, we demonstrated that *IRF1* expression upon DOX-treatment is induced by the DSB sensors ATM/ATR rather than RLR signaling. This induction is independent of CHK1 signaling. Additionally, we identified a previously unappreciated IRF1-depleting effect of the NF-κB inhibitor TPCA-1.

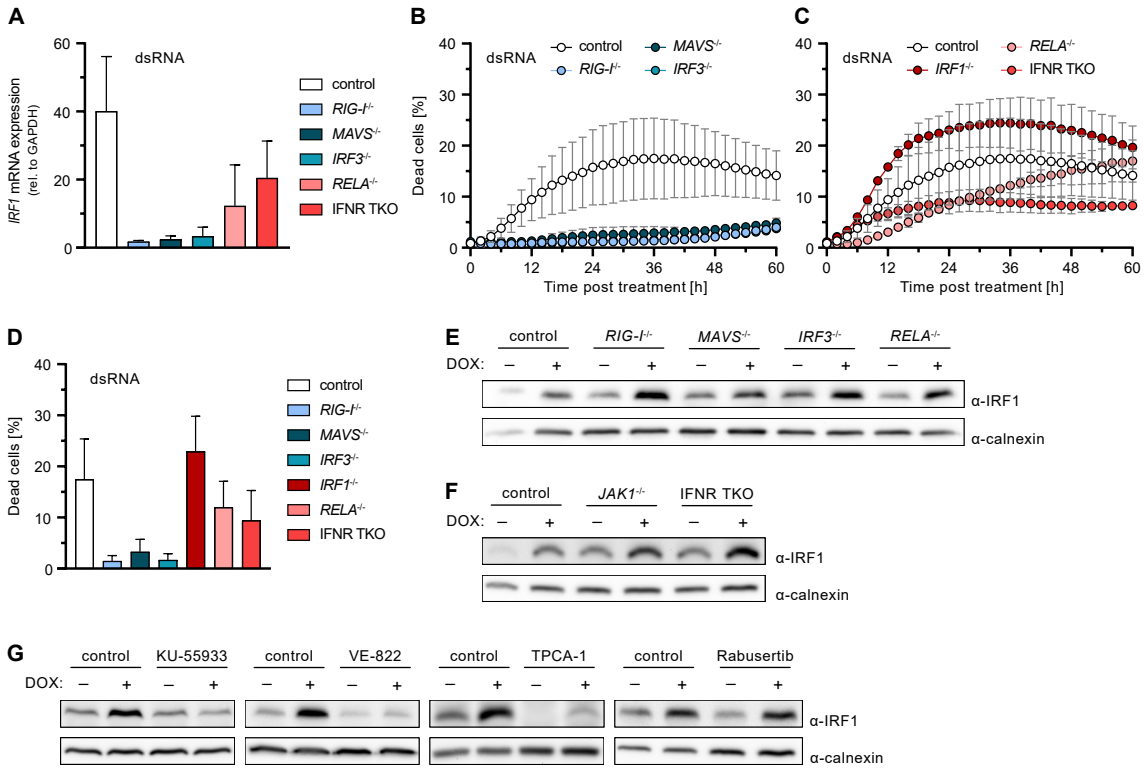

Fig. 5. Effect of cell-intrinsic antiviral signaling components on dsRNA-induced cell death and *IRF1* expression.

(A) A549 cells with functional KO of the indicated genes were stimulated with 2 ng/ml dsRNA for 6 h. IRF1 mRNA transcripts were determined by qRT-PCR. **(B-D)** Percentage of dead A549 cells with functional KO of the indicated genes relative to total cells counted over time **(B, C)** or 36 h **(D)** post dsRNA stimulation. **(E-G)** A549 cells with functional KO of the indicated genes or administration of the indicated inhibitors were treated with

340 2 μM DOX or DMSO for 6 h. Levels of IRF1 were determined by western blot. (**A-D**) Data shown represent the
341 results of at least three biologically independent experiments.

342 **Discussion**

343 Cells, particularly of multicellular organisms, have elaborate systems in place ensuring the integrity of
344 their genome, as DNA damage poses severe risks of accumulating tumorigenic mutations or alterations.
345 In response to excessive DNA damage beyond the potential of being properly repaired, cells trigger the
346 execution of cell death programs, most commonly apoptosis [34]. This is also exploited for common
347 cancer chemoradiotherapies, in which excessive DNA damage is radiologically (e.g., γ-IR) or
348 pharmacologically (e.g., DOX or ETO) introduced, leading to the induction of cell death programs
349 particularly in dividing tissues such as tumors. Elucidating the underlying mechanisms of how DNA
350 damage molecularly leads to cell death is crucial to a better understanding of the circumstances leading
351 to cancer and the pathways relevant for chemoradiotherapy. While classical DNA damage checkpoint
352 control via p53 has been investigated thoroughly [1], much less is known about the relevance and
353 contribution of non-canonical pathways. For example, a ground-breaking study surprisingly found the
354 antiviral type I IFN pathway essential for certain chemotherapies' efficacy [35]. Cytostatic and pro-
355 apoptotic effects of IFNs have long been noticed [36-38]; however, it remained unresolved what
356 triggered the production of IFNs in the studied context in the first place. Recent data also revealed cell-
357 intrinsic triggering of cell death upon activation of antiviral signaling adapters, such as MAVS and
358 STING. Interestingly, this was not only the case for viral infections, but also in response to DNA
359 damage [10, 11, 39].
360 In the present study, we confirm this interrelationship between DNA damage response and antiviral
361 signaling pathways, and we demonstrate an almost complete dependence of DOX- and ETO-triggered
362 cell death on the presence of intact RLR/MAVS signaling. In clear contrast to recently published data,
363 other branches of the cell-intrinsic antiviral defense, such as the TLR or the cGAS/STING system [10,
364 40, 41], did not affect DOX-induced cell death in our experimental setup. Instead, the cytosolic RNA
365 sensors RIG-I and, to a lesser extent, MDA5 were triggered and essential for the induction of cell death.
366 This is in line with a study by Ranoa et al. suggesting small nuclear RNAs U1 and U2 translocate into
367 the cytoplasm in irradiated cells and trigger RIG-I activation [11]. In our experimental system, an intact
368 RIG-I/MDA5-MAVS-IRF3 axis was essential for DNA damage induced cell death; however, we could
369 not observe canonical transcriptional activities of IRF3, such as the induction of IFN genes or ISGs.
370 While the relevance of both IRF3 and p65/RELA suggested the involvement of *IFNB* expression, KO
371 of the receptors for all three types of IFNs (IFNR TKO) did not impact cell death. A plausible
372 mechanism for this IFN-independent triggering of apoptosis is RIPA, involving LUBAC-dependent
373 ubiquitylation of IRF3 and subsequent activation of pro-apoptotic BH3-only proteins [16]. The clear
374 contribution of p65/RELA in our experiments might be through its transcriptional activation of further

375 pro-apoptotic proteins [42]. To our knowledge, cooperative effects between RIPA and NF-κB have not
376 been described before and may be an interesting subject for future investigations.
377 Efficient sensing of nuclear DSBs and triggering an appropriate response is critical for cell survival
378 upon DNA damage, or for initiating cell death and preventing potentially cancerous transformation. As
379 expected, we observed an essential role for p53, highlighting its central function in checkpoint control,
380 coordinating DNA damage repair and triggering apoptosis as a last resort [43]. Interestingly, depletion
381 of p53 reduced the number of apoptotic cells at early time points, but increased cell death at later times.
382 Thus, absence of p53 led to a lack of induction of apoptosis in response to DOX-mediated DSBs at first,
383 but likely massive accumulation of unrepaired DNA damage eventually led to increased, putatively
384 necrotic cell death [44]. As a factor potentially linking the DNA damage response and antiviral
385 signaling, we investigated the role of the multifunctional transcription factor IRF1, as it is known to be
386 involved in both the DNA damage response [8, 25] and IFN signaling [6, 18, 45]. Indeed, we found that
387 *IRF1* was considerably upregulated upon DOX and ETO treatment as well as γ-IR in different cell lines.
388 Interestingly, only in A549 cells, described to be relatively radioresistant as a common characteristic
389 for non-small cellular lung cancers [46], *IRF1* was not appreciably induced upon irradiation. We also
390 observed a reduced histone H2A.X phosphorylation after γ-IR compared to DOX treatment, but
391 potential underlying mechanisms are only partially understood and may comprise several processes [47,
392 48]. Nonetheless, we could further corroborate this clear correlation between *IRF1* induction and
393 triggering/execution of a cell death program on a functional level. Experimentally increasing IRF1
394 levels by stable OE or by pre-treatment of cells with IFN-γ, known as a strong inducer of *IRF1* [45],
395 radioresistance of A549 cells could be overcome. A similar effect has previously been demonstrated in
396 T cells [25]. In our experiments, increased *IRF1* expression also led to a sensitization towards DOX-
397 treatment. *Vice versa, IRF1* KO almost completely rescued cell survival upon DOX-, ETO- and γ-IR-
398 induced DNA damage. These observations clearly establish a fundamentally important role of IRF1 in
399 DNA damage-induced cell death. This is in accordance with literature suggesting IRF1 as a biomarker
400 for radioresistance in tumor cells [49]. For example, extremely radioresistant osteosarcomas were
401 shown to exhibit significantly reduced *IRF1* expression levels [50]. Our data further support
402 establishing IRF1 as a predictive biomarker in chemoradiotherapy in tumor patients.
403 Our finding strongly suggested IRF1 to be the functional link between the DNA damage response and
404 the antiviral system, with RLR signaling (either directly or via the IFN/JAK/STAT cascade) leading to
405 transcriptional activation of IRF1. However, KO experiments clearly refuted this hypothesis. Neither
406 KO of essential factors of the RLR pathway nor of IFN signaling components abolished *IRF1* induction
407 upon DNA damage, suggesting that RLR signaling may activate IRF1 post-translationally. Generally,
408 IRF1 is thought to be only regulated on a transcriptional level [45]. However, one study reports the
409 requirement for "licensing" of IRF1 to become fully active, which required TLR signaling and MYD88
410 [51]. In preliminary experiments, we did not find any evidence for post-translational modifications in
411 our setting, but this may warrant deeper investigations in the future. Alternatively, IRF1 might enhance

412 the transcriptional response of IRF3, as reported before [52]. While we cannot rule out this possibility,
413 the virtually complete inhibition of cell death in *IRF1*$^{-/-}$ despite abundant presence of IRF3 makes this
414 unlikely. In another study, we have also not found any indication of a dampening of IRF3 responses in
415 A549 *IRF1*$^{-/-}$ cells [18]. Notably, despite IRF1 being critically important for cell death induction in our
416 system, *IRF1* (over-)expression alone did not suffice to elicit apoptosis. We therefore suspect RLR
417 signaling and IRF1 activity to cooperate further downstream, putatively via the transcriptional
418 activation of complementary pro-apoptotic factors.
419
420 It is interesting to note that cell death is also elicited upon RLR stimulation by dsRNA (the canonical
421 way to trigger antiviral signaling). Also in this case, *IRF1* is induced, but strictly dependent on RIG-I
422 and to a lesser extent dependent on IFN signaling. Surprisingly, however, depletion of IRF1 did not
423 affect the cell death rate upon dsRNA stimulation, pointing towards transcription-independent
424 mechanisms such as RIPA [15]. Still, KO of NF-κB (*RELA*) or the IFN receptors (IFNR TKO) affect
425 cell death, suggesting some transcriptional regulation, which, however, was independent of IRF1. This
426 may suggest that full-fledged RLR signaling upon dsRNA encounter induces a sufficiently broad
427 transcriptional response, which (in contrast to the situation upon DNA damage) itself is capable of
428 triggering apoptosis. Strikingly, even in dsRNA stimulation, ectopic OE of *IRF1* or pre-treatment of
429 cells with IFN-γ led to a notable increase in the number of dying cells, putatively by the same
430 cooperative pro-apoptotic effects observed in the case of DNA damage. This observation of a general
431 sensitization for cell death by IRF1 is in line with data showing that *IRF1* OE enhances apoptosis in
432 breast or gastric cancer treatment [53-55]. It is further plausible to speculate that reported pro-apoptotic
433 effects of type I IFN [56, 57] would also be mediated by upregulation of *IRF1* through homodimeric
434 STAT1 transcription factor complexes (GAF) inadvertently formed early upon IFNAR engagement
435 [58]. This could mechanistically explain how IFN-α improved chemotherapy response and overall
436 survival in a murine tumor model [35]. Thus, evidence further accumulates suggesting *IRF1*-inducing
437 agents to be more broadly considered as adjuvants in tumor therapy.
438 Two central questions remain: firstly, which pro-apoptotic factors are specifically induced by IRF1
439 upon DNA damage that so potently sensitize cells to committing suicide upon (slight) RLR triggering.
440 To this end, we are currently investigating IRF1-dependent candidate genes induced upon DOX-
441 treatment at a transcriptomic level. Secondly, how is *IRF1* induced upon DNA damage in the first place
442 if not through classical STAT1:STAT1 activity. In our study, we found its transcriptional regulation to
443 be fully independent of RLR signaling and p53 but completely reliant on DNA DSB sensing via ATM
444 and ATR. Still, the downstream pathway leading to *IRF1* expression remains elusive. While p65/RELA
445 or p50/NFKB1 depletion did not affect *IRF1* induction, it was completely abolished by TPCA-1, a
446 commonly known inhibitor of NF-κB. Interestingly, TPCA-1 considerably reduced baseline *IRF1*
447 expression independent of the cell line used, and could even abolish the strong induction upon IFN-γ
448 treatment. Thus, in addition to its inhibitory effects on NF-κB, JAK1, and STAT3 [29, 30, 59], TPCA-

449 1 appears to specifically and very efficiently inhibit the activity of an essential transcription factor for
450 *IRF1*.
451 In conclusion, our study highlights the critical relevance of the antiviral RLR system for the proper and
452 timely induction of cell death upon DNA damage. We provide evidence for independent but cooperative
453 involvement of p53, IRF1 and IRF3 activity upon detection of DNA DSBs by the ATM/ATR
454 machinery. We show that elevating expression levels of *IRF1* lead to the sensitization towards cell death
455 across different genotoxic insults, such as chemotherapeutics, γ-IR or cytosolic dsRNA (i.e. virus
456 infection). These data corroborate a fundamental role for IRF1 and RLR signaling in DNA damage-
457 mediated cell death and suggest future exploration of *IRF1* inducers, such as IFN-γ, together with low-
458 dose RIG-I agonists for their potential as highly efficacious adjuvants in chemoradiotherapy.
459 Additionally, our findings support IRF1 as a biomarker predictive for chemo- and radio-sensitivity of
460 tumors.
461

462 **Literature**

463 1. Sullivan, K.D., et al., *The p53 circuit board.* Biochimica et Biophysica Acta (BBA) -
464 Reviews on Cancer, 2012. **1825**(2): p. 229-244.
465 2. Shiloh, Y. and Y. Ziv, *The ATM protein kinase: regulating the cellular response to*
466 *genotoxic stress, and more.* Nature Reviews Molecular Cell Biology, 2013. **14**(4): p.
467 197-210.
468 3. Shao, L., et al., *Deficiency of the DNA repair enzyme ATM in rheumatoid arthritis.*
469 Journal of Experimental Medicine, 2009. **206**(6): p. 1435-1449.
470 4. Deng, X., et al., *Defective ATM-p53–mediated apoptotic pathway in multiple sclerosis.*
471 Annals of Neurology, 2005. **58**(4): p. 577-584.
472 5. Hecht, F. and B.K. Hecht, *Cancer in Ataxia-telangiectasia patients.* Cancer Genetics
473 and Cytogenetics, 1990. **46**(1): p. 9-19.
474 6. Fujita, T., et al., *Evidence for a nuclear factor(s), IRF-1, mediating induction and*
475 *silencing properties to human IFN-beta gene regulatory elements.* The EMBO Journal,
476 1988. **7**(11): p. 3397-3405.
477 7. Yamane, D., et al., *Basal expression of interferon regulatory factor 1 drives intrinsic*
478 *hepatocyte resistance to multiple RNA viruses.* Nature Microbiology, 2019. **4**(7): p.
479 1096-1104.
480 8. Harada, H., et al., *Anti-oncogenic and oncogenic potentials of interferon regulatory*
481 *factors-1 and -2.* Science, 1993. **259**(5097): p. 971.
482 9. Doherty, G.M., et al., *Interferon regulatory factor expression in human breast cancer.*
483 Annals of surgery, 2001. **233**(5): p. 623-629.
484 10. Härtlova, A., et al., *DNA Damage Primes the Type I Interferon System via the Cytosolic*
485 *DNA Sensor STING to Promote Anti-Microbial Innate Immunity.* Immunity, 2015.
486 **42**(2): p. 332-343.
487 11. Ranoa, D.R.E., et al., *Cancer therapies activate RIG-I-like receptor pathway through*
488 *endogenous non-coding RNAs.* Oncotarget, 2016. **7**(18): p. 26496-26515.
489 12. Elion, D.L., et al., *Therapeutically Active RIG-I Agonist Induces Immunogenic Tumor*
490 *Cell Killing in Breast Cancers.* Cancer Research, 2018. **78**(21): p. 6183.
491 13. Besch, R., et al., *Proapoptotic signaling induced by RIG-I and MDA-5 results in type I*
492 *interferon–independent apoptosis in human melanoma cells.* The Journal of Clinical
493 Investigation, 2009. **119**(8): p. 2399-2411.

494 14. Goubau, D., et al., *Transcriptional re-programming of primary macrophages reveals*
495 *distinct apoptotic and anti-tumoral functions of IRF-3 and IRF-7.* European Journal of
496 Immunology, 2009. **39**(2): p. 527-540.
497 15. Chattopadhyay, S., et al., *Viral apoptosis is induced by IRF-3-mediated activation of*
498 *Bax.* The EMBO Journal, 2010. **29**(10): p. 1762-1773.
499 16. Chattopadhyay, S., et al., *Ubiquitination of the Transcription Factor IRF-3 Activates*
500 *RIPA, the Apoptotic Pathway that Protects Mice from Viral Pathogenesis.* Immunity,
501 2016. **44**(5): p. 1151-1161.
502 17. El Maadidi, S., et al., *A Novel Mitochondrial MAVS/Caspase-8 Platform Links RNA*
503 *Virus–Induced Innate Antiviral Signaling to Bax/Bak-Independent Apoptosis.* The
504 Journal of Immunology, 2014. **192**(3): p. 1171.
505 18. Wüst, S., et al., *Comparative Analysis of Six IRF Family Members in Alveolar*
506 *Epithelial Cell-Intrinsic Antiviral Responses.* Cells, 2021. **10**(10): p. 2600.
507 19. Willemsen, J., et al., *Phosphorylation-Dependent Feedback Inhibition of RIG-I by*
508 *DAPK1 Identified by Kinome-wide siRNA Screening.* Molecular Cell, 2017. **65**(3): p.
509 403-415.e8.
510 20. Krischuns, T., et al., *Phosphorylation of TRIM28 Enhances the Expression of IFN-β*
511 *and Proinflammatory Cytokines During HPAIV Infection of Human Lung Epithelial*
512 *Cells.* Front Immunol, 2018. **9**: p. 2229.
513 21. Urban, C., et al., *Persistent Innate Immune Stimulation Results in IRF3-Mediated but*
514 *Caspase-Independent Cytostasis.* Viruses, 2020. **12**(6).
515 22. Bender, S., et al., *Activation of Type I and III Interferon Response by Mitochondrial*
516 *and Peroxisomal MAVS and Inhibition by Hepatitis C Virus.* PLOS Pathogens, 2015.
517 **11**(11): p. e1005264.
518 23. Binder, M., et al., *Molecular mechanism of signal perception and integration by the*
519 *innate immune sensor retinoic acid-inducible gene-I (RIG-I).* The Journal of biological
520 chemistry, 2011. **286**(31): p. 27278-27287.
521 24. Wang, S., et al., *Doxorubicin induces apoptosis in normal and tumor cells via distinctly*
522 *different mechanisms. intermediacy of H(2)O(2)- and p53-dependent pathways.* J Biol
523 Chem, 2004. **279**(24): p. 25535-43.
524 25. Tamura, T., et al., *An IRF-1-dependent pathway of DNA damage-induced apoptosis in*
525 *mitogen-activated T lymphocytes.* Nature, 1995. **376**(6541): p. 596-599.

526 26. Hickson, I., et al., *Identification and Characterization of a Novel and Specific Inhibitor*
527 *of the Ataxia-Telangiectasia Mutated Kinase ATM.* Cancer Research, 2004. **64**(24): p.
528 9152.
529 27. Fokas, E., et al., *Targeting ATR in vivo using the novel inhibitor VE-822 results in*
530 *selective sensitization of pancreatic tumors to radiation.* Cell Death & Disease, 2012.
531 **3**(12): p. e441-e441.
532 28. Tong, A.-J., et al., *A Stringent Systems Approach Uncovers Gene-Specific Mechanisms*
533 *Regulating Inflammation.* Cell, 2016. **165**(1): p. 165-179.
534 29. Cataldi, M., et al., *Breaking resistance of pancreatic cancer cells to an attenuated*
535 *vesicular stomatitis virus through a novel activity of IKK inhibitor TPCA-1.* Virology,
536 2015. **485**: p. 340-354.
537 30. Podolin, P.L., et al., *Attenuation of Murine Collagen-Induced Arthritis by a Novel,*
538 *Potent, Selective Small Molecule Inhibitor of IκB Kinase 2, TPCA-1 (2-*
539 *[(Aminocarbonyl)amino]-5-(4-fluorophenyl)-3-thiophenecarboxamide), Occurs via*
540 *Reduction of Proinflammatory Cytokines and Antigen-Induced T Cell Proliferation.*
541 Journal of Pharmacology and Experimental Therapeutics, 2005. **312**(1): p. 373.
542 31. Bartek, J. and J. Lukas, *Chk1 and Chk2 kinases in checkpoint control and cancer.*
543 Cancer Cell, 2003. **3**(5): p. 421-429.
544 32. Schmitt, Adam M., et al., *p50 (NF-κB1) Is an Effector Protein in the Cytotoxic*
545 *Response to DNA Methylation Damage.* Molecular Cell, 2011. **44**(5): p. 785-796.
546 33. King, C., et al., *Characterization and preclinical development of LY2603618: a*
547 *selective and potent Chk1 inhibitor.* Investigational New Drugs, 2014. **32**(2): p. 213-
548 226.
549 34. Norbury, C.J. and B. Zhivotovsky, *DNA damage-induced apoptosis.* Oncogene, 2004.
550 **23**(16): p. 2797-2808.
551 35. Sistigu, A., et al., *Cancer cell–autonomous contribution of type I interferon signaling*
552 *to the efficacy of chemotherapy.* Nature Medicine, 2014. **20**: p. 1301.
553 36. Balkwill, F., D. Watling, and J. Taylor-Papadimitriou, *Inhibition by lymphoblastoid*
554 *interferon of growth of cells derived from the human breast.* International Journal of
555 Cancer, 1978. **22**(3): p. 258-265.
556 37. Widau, R.C., et al., *RIG-I–like receptor LGP2 protects tumor cells from ionizing*
557 *radiation.* Proceedings of the National Academy of Sciences, 2014. **111**(4): p. E484.

558 38. Chiappinelli, Katherine B., et al., *Inhibiting DNA Methylation Causes an Interferon*
559 *Response in Cancer via dsRNA Including Endogenous Retroviruses.* Cell, 2015. **162**(5):
560 p. 974-986.
561 39. Guo, Q., et al., *STING promotes senescence, apoptosis, and extracellular matrix*
562 *degradation in osteoarthritis via the NF-κB signaling pathway.* Cell Death & Disease,
563 2021. **12**(1): p. 13.
564 40. Harberts, E., et al., *MyD88 mediates the decision to die by apoptosis or necroptosis*
565 *after UV irradiation.* Innate Immunity, 2013. **20**(5): p. 529-539.
566 41. Huang, T.T., et al., *Sequential Modification of NEMO/IKKγ by SUMO-1 and Ubiquitin*
567 *Mediates NF-κB Activation by Genotoxic Stress.* Cell, 2003. **115**(5): p. 565-576.
568 42. Wang, P., et al., *PUMA is directly activated by NF-κB and contributes to TNF-α-*
569 *induced apoptosis.* Cell Death & Differentiation, 2009. **16**(9): p. 1192-1202.
570 43. Gatz, S.A. and L. Wiesmüller, *p53 in recombination and repair.* Cell Death &
571 Differentiation, 2006. **13**(6): p. 1003-1016.
572 44. Boege, Y., et al., *A Dual Role of Caspase-8 in Triggering and Sensing Proliferation-*
573 *Associated DNA Damage, a Key Determinant of Liver Cancer Development.* Cancer
574 Cell, 2017. **32**: p. 342 - 359.e10.
575 45. Feng, H., et al., *Interferon regulatory factor 1 (IRF1) and anti-pathogen innate immune*
576 *responses.* PLOS Pathogens, 2021. **17**(1): p. e1009220.
577 46. Kim, W., et al., *PIM1-Activated PRAS40 Regulates Radioresistance in Non-small Cell*
578 *Lung Cancer Cells through Interplay with FOXO3a, 14-3-3 and Protein Phosphatases.*
579 Radiation Research, 2011. **176**(5): p. 539-552.
580 47. Yang, H.J., et al., *Investigation of Radiation-induced Transcriptome Profile of*
581 *Radioresistant Non-small Cell Lung Cancer A549 Cells Using RNA-seq.* PLOS ONE,
582 2013. **8**(3): p. e59319.
583 48. Pawlik, A., et al., *Transcriptome Characterization Uncovers the Molecular Response*
584 *of Hematopoietic Cells to Ionizing Radiation.* Radiation Research, 2010. **175**(1): p. 66-
585 82.
586 49. Zhang, Q., et al., *Integrating radiosensitive genes improves prediction of*
587 *radiosensitivity or radioresistance in patients with oesophageal cancer.* Oncology
588 letters, 2019. **17**(6): p. 5377-5388.
589 50. Jones, K.B., et al., *miRNA signatures associate with pathogenesis and progression of*
590 *osteosarcoma.* Cancer research, 2012. **72**(7): p. 1865-1877.

591 51. Negishi, H., et al., *Evidence for licensing of IFN-γ-induced IFN regulatory factor 1*
592 *transcription factor by MyD88 in Toll-like receptor-dependent gene induction*
593 *program.* Proceedings of the National Academy of Sciences, 2006. **103**(41): p. 15136.
594 52. Wang, J., et al., *IRF1 Promotes the Innate Immune Response to Viral Infection by*
595 *Enhancing the Activation of IRF3.* Journal of Virology, 2020. **94**(22): p. e01231-20.
596 53. Bouker, K.B., et al., *Interferon regulatory factor-1 (IRF-1) exhibits tumor suppressor*
597 *activities in breast cancer associated with caspase activation and induction of*
598 *apoptosis.* Carcinogenesis, 2005. **26**(9): p. 1527-1535.
599 54. Kim, P.K.M., et al., *IRF-1 expression induces apoptosis and inhibits tumor growth in*
600 *mouse mammary cancer cells in vitro and in vivo.* Oncogene, 2004. **23**(5): p. 1125-
601 1135.
602 55. Tan, L., et al., *Interferon regulatory factor-1 suppresses DNA damage response and*
603 *reverses chemotherapy resistance by downregulating the expression of RAD51 in*
604 *gastric cancer.* Am J Cancer Res, 2020. **10**(4): p. 1255-1270.
605 56. Thyrell, L., et al., *Mechanisms of Interferon-alpha induced apoptosis in malignant*
606 *cells.* Oncogene, 2002. **21**(8): p. 1251-1262.
607 57. Choi, E.A., et al., *Stat1-dependent Induction of Tumor Necrosis Factor-related*
608 *Apoptosis-inducing Ligand and the Cell-Surface Death Signaling Pathway by*
609 *Interferon β in Human Cancer Cells.* Cancer Research, 2003. **63**(17): p. 5299.
610 58. Kok, F., et al., *Disentangling molecular mechanisms regulating sensitization of*
611 *interferon alpha signal transduction.* Molecular systems biology, 2020. **16**(7): p.
612 e8955-e8955.
613 59. Nan, J., et al., *TPCA-1 Is a Direct Dual Inhibitor of STAT3 and NF-κB and Regresses*
614 *Mutant EGFR-Associated Human Non–Small Cell Lung Cancers.* Molecular Cancer
615 Therapeutics, 2014. **13**(3): p. 617.

616